



# Rational Design of Glycomimetic Compounds Targeting the *Saccharomyces cerevisiae* Transglycosylase Gas2

Ignacio Delso<sup>1,2,\*</sup>, Jessika Valero-González<sup>3</sup>, Eduardo Marca<sup>1</sup>, Tomás Tejero<sup>1</sup>, Ramón Hurtado-Guerrero<sup>3,4,\*</sup> and Pedro Merino<sup>1,\*</sup>

<sup>1</sup>Laboratorio de Síntesis Asimétrica, Departamento de Síntesis y Estructura de Biomoléculas, Instituto de Síntesis Química y Catálisis Homogénea (ISQCH), CSIC, Universidad de Zaragoza, Zaragoza, Aragón 50009, Spain

<sup>2</sup>Servicio de Resonancia Magnética Nuclear, Centro de Química y Materiales de Aragón (CEQMA), CSIC, Universidad de Zaragoza, Campus San Francisco, Zaragoza, Aragón 50009, Spain

<sup>3</sup>Instituto de Biocomputación y Física de Sistemas Complejos (BIFI), BIFI-IQFR (CSIC) Joint Unit, Universidad de Zaragoza, Zaragoza, Aragón 50009, Spain

<sup>4</sup>Fundación ARAID, Gobierno de Aragón, Zaragoza, Aragón 50009, Spain

\*Corresponding authors: Ignacio Delso, [idelso@unizar.es](mailto:idelso@unizar.es); Ramón Hurtado-Guerrero, [rhurtado@bifi.es](mailto:rhurtado@bifi.es); Pedro Merino, [pmerino@unizar.es](mailto:pmerino@unizar.es)

The transglycosylase *Saccharomyces cerevisiae* Gas2 (ScGas2) belongs to a large family of enzymes that are key players in yeast cell wall remodeling. Despite its biologic importance, no studies on the synthesis of substrate-based compounds as potential inhibitors have been reported. We have synthesized a series of docking-guided glycomimetics that were evaluated by fluorescence spectroscopy and saturation-transfer difference (STD) NMR experiments, revealing that a minimum of three glucose units linked via a  $\beta$ -(1,3) linkage are required for achieving molecular recognition at the binding donor site. The binding mode of our compounds is further supported by STD-NMR experiments using the active site-mutants Y107Q and Y244Q. Our results are important for both understanding of ScGas2–substrate interactions and setting up the basis for future design of glycomimetics as new antifungal agents.

**Key words:** carbohydrates, docking, glycomimetics, STD-NMR, transglycosylases

Received 2 July 2015, revised 1 August 2015 and accepted for publication 11 August 2015

Enzymes that can transfer single or multiple activated carbohydrate units to a range of substrates are involved in important biologic processes and therefore are potential

pharmaceutical targets (1,2). In particular, transglycosylases that belong to GH72 in the CAZy database (3) are ubiquitous enzymes present in fungal organisms. These glycosylphosphatidylinositol (GPI)-anchored enzymes are crucial for remodeling of fungal cell wall (4,5), which is an essential structure in scaffolding the cytoplasmic membrane and maintaining structural integrity of those microorganisms. While some information about the enzymes responsible for the cell wall biosynthesis is available (6–10), little is known of the involvement of these transglycosylases in the construction and remodeling of the fungal cell wall (11).

These transglycosylases are classified as glycosyl hydrolases due to their typical folding, which consists of a TIM barrel domain formed by  $(\beta\alpha)_8$  (12,13). Although the overall structure resembles a glycosyl hydrolase, its activity shows a balance among hydrolysis and transglycosylation depending on the length of the substrate. For example, *Saccharomyces cerevisiae* Gas2 (ScGas2; Figure 1) is inactive against laminaripentaose (G5) but is a pure hydrolase against laminarihexaose and heptaose and becomes a transglycosylase against larger sized laminarioligosaccharides (13). In the case of *Aspergillus fumigatus* Gel1, laminarinonaose was the minimal tested size to have transglycosylase activity (14). Several efforts have been made on elucidating the mechanism of action of transglycosylases (15–18), and several antibiotics that inhibit the transglycosylation step in bacteria have been designed (19).

This family of fungal enzymes has key important biologic roles in yeast and fungi and in some cases are even essential for pathogens such as *Aspergillus fumigatus* (20). Consequently, the targeting of these enzymes with specific inhibitors might represent potential therapies to treat selectively fungi-related pathologies such as Aspergillosis and Candidiasis that constitute important current medical problems (21–29).

Despite of their biologic importance, the unique enzyme from this family whose tridimensional structure is described is ScGas2. Several X-ray structures have been resolved (13), including the apo-structure (E176Q mutant, PDB entry 2W61) and structures in complex with laminaripentaose (PDB entry 2W62) and with laminaritriose and

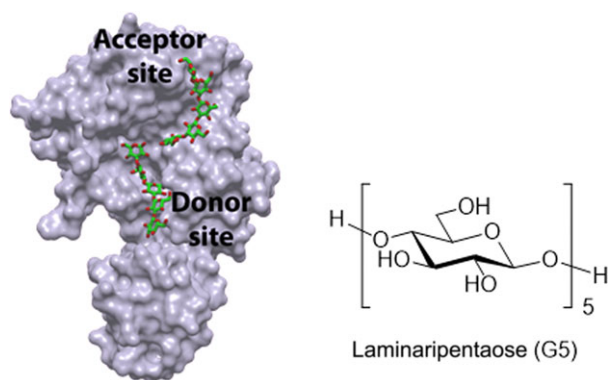


**Figure 1:** Surface representation of ScGas2 in complex with two G5 units at donor (positions  $-5$  to  $-1$ ) and acceptor (positions  $+1$  to  $+5$ ) sites.

laminaripentaose (PDB entry 2W63). From these crystallographic data, the architecture of this family of enzymes was described and their catalytic mechanism was proposed. The active site of ScGas2 shows two catalytic residues, the nucleophile E275 and the acid-base E176, and four well-conserved tyrosine residues (Y107, Y244, Y307, and Y316). To explain the transglycosylation mechanism, the ‘base occlusion mechanism’ was proposed, in which the leaving hydrolyzed sugar blocks the entrance of a key water molecule and thus avoids hydrolysis, favoring transglycosylation (13).

Our aim was to design glycomimetics as potential inhibitors targeting essential transglycosylases of the fungal cell wall. In particular, it is well known that Gel4, a homologue of ScGas2, is essential in *Asp. fumigatus*, and consequently, the design of glycomimetics for this enzyme might become future drugs to treat Aspergillosis. Due to that we could only express and purify ScGas2, we decided to use ScGas2 as a template for AfGel4. The study of the identity between ScGas2 and different homologues was already reported (13), and from these data, it was very clear that overall all members of this family conserve all the important residues involved in catalysis and sugar recognition. Of note, ScGas2 might serve as a template to discover inhibitors for AfGel4 given the high identity among them at the active site level (the identity between the catalytic domains is  $\sim 50\%$  and reaches  $100\%$  when all the key residues recognizing the carbohydrates from  $-3$  to  $+1$  are considered). This makes ScGas2 very appealing for the design of new glycomimetics not only targeting ScGas2 but also AfGel4. Recently, we developed a synthetic strategy for the preparation of O- and C-glycosides derived from  $\beta$ -(1,3)-D-glucans (30) that demonstrated its utility for the synthesis of di- and trisaccharide analogues.

Herein, we have further explored the combination of different radicals covalently bound to variable laminooligosaccharides; in particular, we fixed our attention on compounds **1–3** (Figure 2). The interactions of these compounds with ScGas2 were analyzed by computational

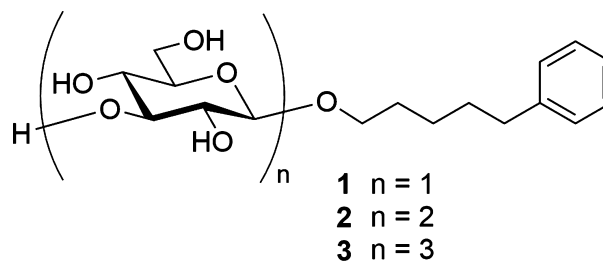


**Figure 2:** O-glycosides derived from  $\beta$ -(1,3)-D-glucans.

molecular docking studies, STD-NMR experiments and tryptophan fluorescence spectroscopy, and applied this information to unambiguously determine the minimal substrate length required for the design and synthesis of glycomimetics for the ScGas2 enzyme.

## Methods and Materials

### NMR studies

NMR spectra were recorded in a Bruker 500 MHz spectrometer, equipped with a direct TBO probe.  $^1\text{H}$  spectra were recorded with water signal suppression using excitation sculpting with gradients (Pulse program zgesgp). Water saturation pulse was adjusted to 2 ms with a Sinc1.1000 shape. Saturation-transfer difference spectra were acquired with water suppression using excitation sculpting with gradients (Pulse program stddiffesgp.3). Protein saturation pulse was adjusted to 50 ms, with an Eburp2.1000 shape during 2 seconds. Saturation frequency was optimized to  $-0.5$  ppm when on resonance and 40 ppm when off-resonance. Relaxation delay was adjusted to 1.5 seconds and acquisition time to 2.5 seconds. For both on- and off-resonance, 1024 spectra were acquired. Sample temperature was fixed to 298 K. All measured samples were prepared on deuterated-TRIS 25 mm in deuterium oxide at pH 8.0, dissolving ligand to 1 mM and corresponding protein to 20  $\mu\text{M}$ . STD spectra were recorded with separated solution components to check blank. Only protein signals between 1.25 and 0.50 ppm appear as background, and the TRIS signal at 3.60 ppm.

### Docking studies

Compounds **1–3** were docked into the catalytic site of ScGas2 (PDB ID 2W62) using Glide software from Schrödinger. Protein was prepared with the Protein Preparation Wizard, and the water molecules and the acceptor oligosaccharide were removed. Grid was prepared with a box size of  $45 \times 45 \times 45 \text{ \AA}$ , centered on the donor oligosaccharide, using OPLS-2005 force field. Ligands were designed with Maestro, prepared with LigPrep, and minimized using Gaussian 09 (31), with a convergence threshold of 0.05 and 5000 maximum iterations. Afterward, MacroModel was used to generate 1000 different conformations for each ligand. Glide was run on XP mode (Extra Precision) using as input all calculated conformations.

Schrödinger Suite 2013 was used for all computational calculations: MAESTRO 9.4 for viewing and protein preparation; LIGPREP 2.6 for ligand preparation; MACROMODEL 10.0 for ligand energy minimization; GLIDE 5.9 for molecular docking.

### Cloning, expression, and purification

The cloning was carried out as described before (13) with the exception that the DNA sequence encoding to the amino acids residues 26–525 of the *S. cerevisiae* Gas2 which was obtained by PCR from the *S. cerevisiae* strain BY4741 kindly provided by Prof. Javier Arroyo (Universidad Complutense de Madrid, Spain). The double mutant N498D/N510D, referred to here as the wild type, and the mutants Y244Q and Y107Q were also generated as shown before (13).

The expression system used was *Pichia Pastoris* strain X33 (Invitrogen, Grand Island, NY, USA). Batch cultures were performed in 1 liter of BMGY medium (1% (w/v) yeast extract, 2% (w/v) peptone, 100 mM potassium phosphate (pH 6.0), 1.34% (w/v) yeast nitrogen based and 1% (v/v) glycerol) overnight at 30 °C, then centrifuged at 4000 *g* for 10 min. Cells were resuspended in BMMY medium (1% (w/v) yeast extract, 2% (w/v) peptone, 100 mM potassium phosphate pH 6.0, 1.34% (w/v) yeast nitrogen base, and 1% (v/v) methanol) and incubated at 18 °C. Supernatant containing ScGas2 and mutants was collected after 72 h of methanol induction and concentrated to 20–50 mL using a Pellicon XL device (Millipore, Billerica, MA, USA), and dialyzed against 25 mM Tris and 5 mM sodium phosphate pH 7.5. Samples were loaded into 1 × 5 mL CHT Type I cartridge (Bio-Rad, Hercules, CA, USA), previously equilibrated with 25 mM Tris and 5 mM sodium phosphate pH 7.5. The protein was eluted with a sodium phosphate gradient (5–500 mM). Gel filtration was carried out using SUPERDEX 75 XK26/60 column in buffer containing 25 mM Tris pH 7.5 and 150 mM NaCl. The protein was dialyzed in Tris–HCl 25 mM pH 7.5.

### Fluorescence spectroscopy assay

Fluorescence spectroscopy assay was carried out to evaluate the dissociation constants of ScGas2 WT against compounds **1–3**. These experiments were conducted in a Cary Eclipse spectrofluorometer (Varian, Palo Alto, CA, USA) at 25 °C. Protein concentration was 1 μM in every case, and concentration of compounds **1–3** varied from 0.1 to 4 mM in buffer 25 mM Tris pH 7.5. Fluorescence emission spectra were registered in the 300–450 nm range with an excitation wavelength of 280 nm.

Data analysis was performed in Prism (GraphPad Software Inc., La Jolla, CA, USA) according to the fitting equation below:

$$1 - \frac{F_i}{F_0} = \frac{f_k[Q]}{K_d + [Q]}$$

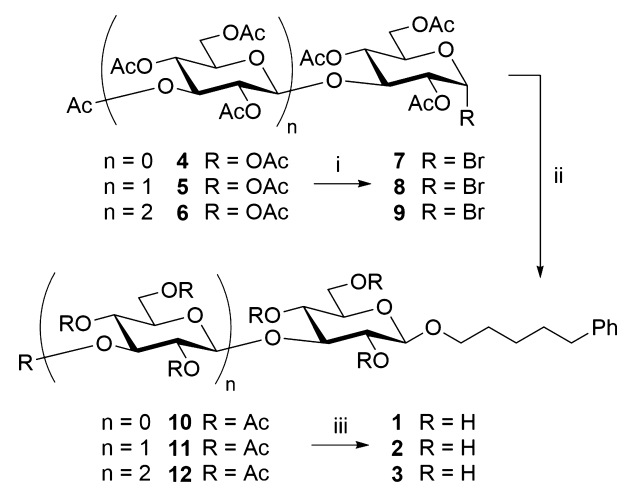
### Inhibition assays

Activity was measured monitoring laminarihexaose (G6) hydrolysis obtaining as major products laminaritetraose, laminaritriose, and laminaribiose. Reactions took place at 30 °C on a final volume of 100 μL of ammonium formate-buffered solution (10 mM) at pH 5.5, containing fixed concentrations of ScGas2 (5 μM) and G6 (0.5 mM, Megazyme, Ireland) and variable concentrations of compound **3** (100, 200 and 500 μM, 1, 2 and 5 mM). Reaction was monitored every 30 min, over 3 h, with two repetitions. Hydrolysis ratio was determined by comparison of G6 concentration (mean of two measurements). IC50 was calculated by extrapolating the inhibitor concentration at which G6 hydrolysis is half of obtained in absence of compound **3**.

Oligosaccharides were determined by UPLC chromatography on a 2.1 mm i.d. × 50 mm ACQUITY 1.7 μM BEH Amide (Waters Corp, Milford, MA, USA) using an ACQUITY UPLC system (Waters Corp). The column was maintained at 35 °C. Mobile phase, at a flow rate of 0.800 mL/min, consisted of 68% acetonitrile and 32% water, both solvents doped with 0.2% triethylamine. One microlitre of sample was injected without any pretreatment. Carbohydrates were detected with an Evaporative Light Scattering Detector (ELSD; Waters Corp) with optimized conditions as follows: temperature of drift tube 100 °C, nebulizer temperature 45 °C, gain 1000, and nitrogen pressure 30 psi. G6 retention time, on these conditions, is 58–62 seconds.

### Results

Compounds **1–3** were prepared by glycosylation of the corresponding glycosyl bromide, derived from peracetylated laminarioligosaccharide following the procedure we described previously (30) (Scheme 1). Spectroscopic data



**Scheme 1:** Synthesis of compounds **1–3**. (i) 30% HBr, AcOH, rt, 15 min (76%). (ii) Ph(CH<sub>2</sub>)<sub>5</sub>OH, AgCO<sub>3</sub>, CH<sub>2</sub>Cl<sub>2</sub>, rt, 20 h (63%). (iii) NaOMe, MeOH, rt, 4 h (quant.).

for compounds **1–3**, as well as for intermediates, are available in the Appendix S1.

Docking studies were initially performed with G5 on the entire enzyme ScGas2 (PDB code 2W62) using the Schrödinger Software (32–34). Analogous studies were carried out with glycomimetics **1–3**, and the best affinity was observed for compound **3**. Differences of ca. 9 and 4 kcal/mol were found between the lowest energy representative cluster for compound **3** and for compounds **1** and **2**, respectively (Figure 3). Calculations with **1–3**

revealed notable differences in binding energy for each derivative with ScGas2. Furthermore, poses obtained for each compound showed a different dispersion on their geometry. In particular, compound **3** showed lower pose dispersion around the minimum energy pose.

STD-NMR experiments (35,36) were measured on the corresponding ligand and ScGas2 mixtures. STD-NMR spectra showed depreciable signal for compound **1** (Figure 4, traces A and B), but a slight STD signal for compound **2** (Figure 4, traces C and D). In this latter case, a STD signal

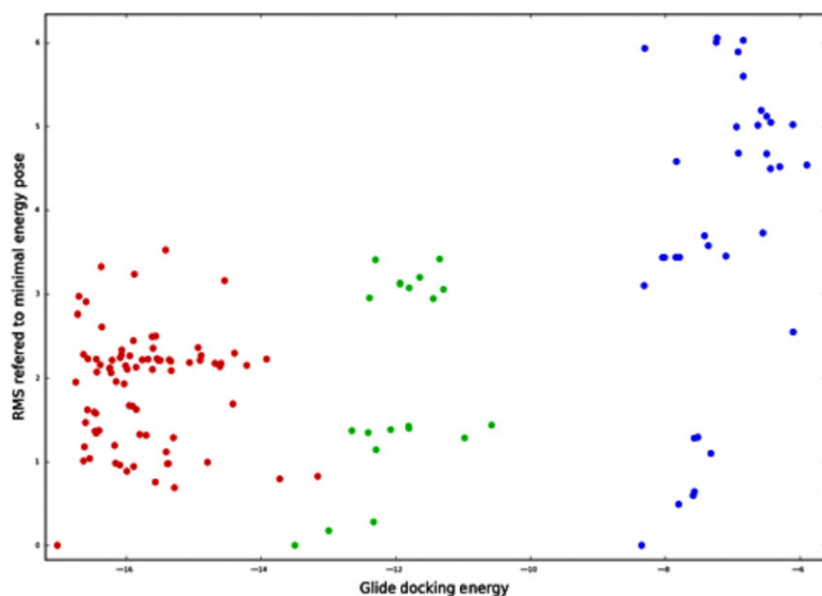


**Figure 3:** Graphical representation of Glide Docking Energy (Kcal/mol) versus RMSD calculated from the lowest energy pose for each product, being **1** (blue), **2** (green), and **3** (red).

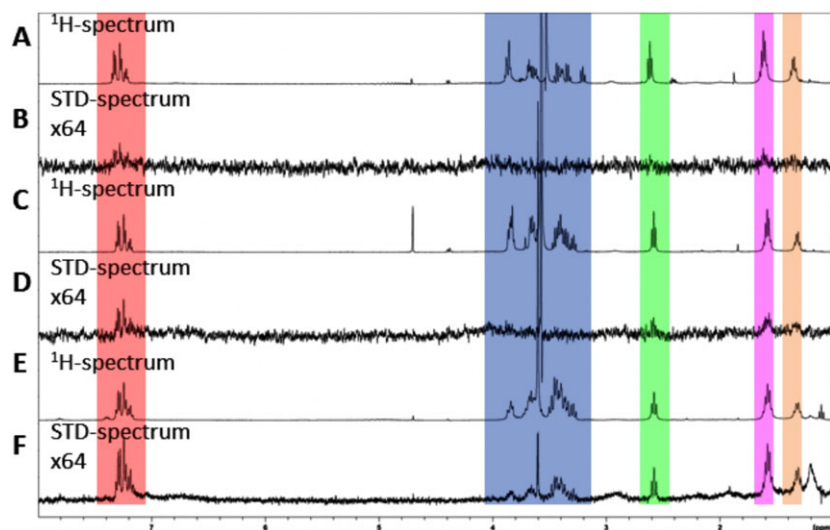
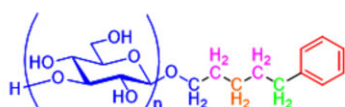


**Figure 4:**  $^1\text{H}$  spectra and STD-NMR spectra measured for compounds **1–3**. STD spectra are scaled up 64 times. Traces A and B correspond to compound **1**; traces C and D correspond to compound **2**; traces E and F correspond to compound **3**.

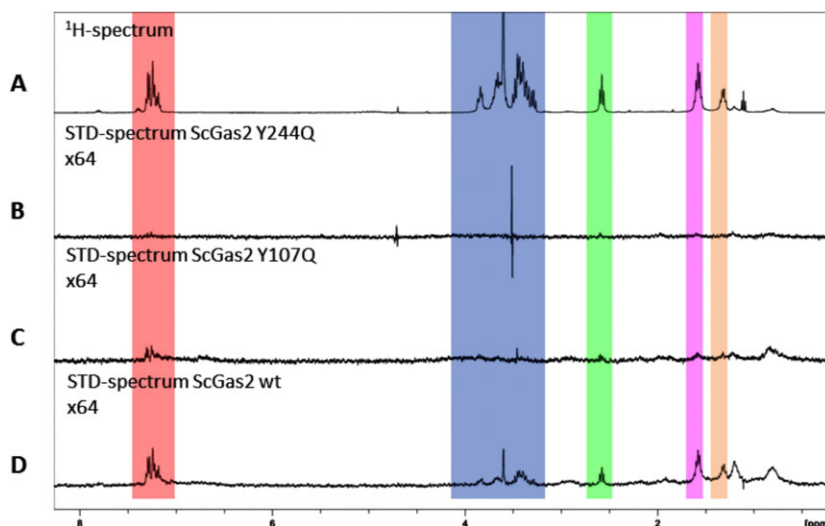


**Figure 5:** STD-NMR spectra for Y244Q mutant (trace B), Y107Q mutant (trace C), and the wild-type enzyme (trace D) with **3**.  $^1\text{H}$  NMR spectrum of compound **3** is given in trace A.

corresponding to aromatic protons, with an enhancement of 1%, could be observed; methylene groups showed an enhancement below 1%. On the other hand, no STD signal was observed for glucose moieties. STD spectrum for compound **3** showed more intense signals for the whole molecule than the other two compounds (Figure 4, traces E and F). Under the same conditions, both the aromatic ring and the pentyl spacer showed an enhancement of 3%. Laminaritriose signal showed a STD enhancement of 1% (except those lost due to solvent suppression).

A comparison of the STD-NMR experiments carried out with the wild-type protein (Figure 5, trace D), and mutants Y244Q (Figure 5, trace B) and Y107Q (Figure 5, trace C), shows a complete disappearance of STD signals for the Y244Q

mutant, and an enhancement below 1% for aromatic and methylene protons when Y107Q mutant is present.

Tryptophan fluorescence studies (Figure 6) provided for compound **3**  $K_d$  of  $800 \pm 100 \mu\text{M}$ . Unlike compound **3**, compounds **1** and **2** did not show dose-response changes impeding to obtain  $K_d$  values.

Inhibition data were obtained by measuring the hydrolytic activity of the enzyme. Laminarihexose (G6) has been used as the substrate for hydrolysis, mainly rendering laminaribiose, laminaritriose, and laminartetraose without any measurable transglycosylation activity (13). Determination of the hydrolytic activity of ScGas2 in the presence of compound **3** rendered an  $\text{IC}_{50}$  value of 1.55 mM. No effects on laminarihexaose hydrolysis were observed when **1** and **2** were added to the reaction. An additional reaction was monitored containing **3** (2 mM) and ScGas2, in the

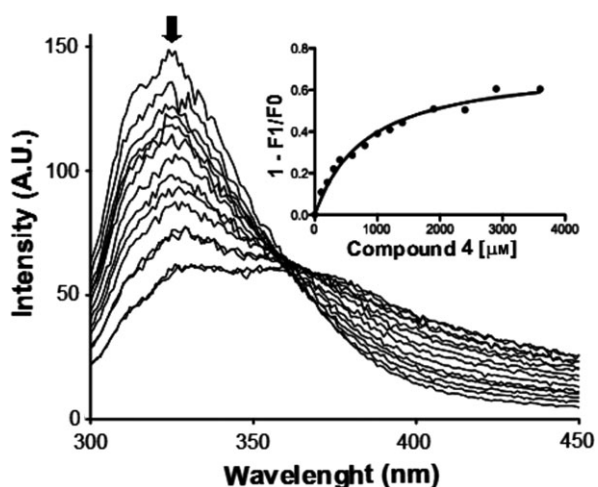


**Figure 6:** Quenching of intrinsic ScGas2 tryptophan fluorescence measured at increasing concentrations of the compound **3**. All data points represent the means  $\pm$  SD for three measurements. The  $K_d$  for compound **3** was determined by fitting fluorescence intensity data against compound **3** concentration.

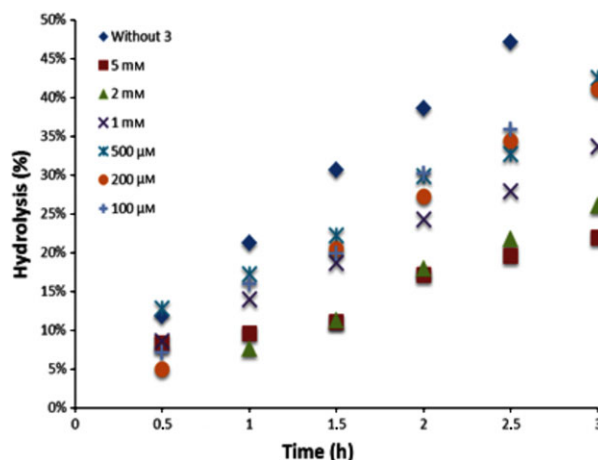


**Figure 7:** Evolution of G6 hydrolysis in the presence **3** in different concentrations.

absence of substrate (G6). No evolution was observed over 24 h at 30 °C (Figure 7).

## Discussion

Docking results clearly match the previously described binding mode of G5 (13) (RMSD of 0.35 and 0.12 Å for sugars adopting the lowest representative energy cluster located from  $-5$  to  $-1$ , and  $+5$  to  $+1$ , respectively) and reveal a higher affinity of G5 for the donor site than for the acceptor site of the protein (Figure 8, top panel). Indeed, a strong correlation is observed between the G5 binding mode with the lower energy calculated poses. These docking studies showed that the conformation of residues in positions  $-2$  and  $-3$  did not change to a large extent, remaining fixed by several H-bond interactions (Figure 8, bottom panel).

On the other hand, residues on  $-4$  and  $-5$  positions, located far from the reaction site, show higher flexibility in all studied conformations. Residue on position  $-1$  is involved in CH- $\pi$  interactions with the phenyl ring of amino acid residue Y107 and a key H-bond with hydroxyl group on residue Y307. In addition, the reaction site is also characterized by the presence of a hydrophobic pocket formed by the side chains of residues Y244, Y307, and Y316. Thus, our *in silico*

study allowed us to conclude that the enzyme shows higher affinity for sugars at position  $-3$  and  $-2$ , suggesting that potential glycomimetics should contain at least 2 units of glucose, specifically  $\beta$ -(1,3) bonded. The presence of that hydrophobic pocket prompted us to consider glycomimetics containing aromatic radicals, such as compounds **1–3**, as good candidates for binding the active site.

The most representative poses obtained from docking studies for compounds **1–3** are illustrated in Figure 9 (top panel). In all cases, the carbohydrate units remain at the donor site. Compound **3** is the only one occupying positions  $-1$  to  $-3$ , as found for the natural substrate. In fact, calculated RMSD for the carbohydrate moiety between laminaripentaose from the PDB entry 2W62 and compound **3** is 0.174 Å, being the maximum deviation of 0.291 Å. Furthermore, the fact of **3** occupying the  $-1$  position with the functionalized ring allows the phenylpentyl moiety to overpass catalytic residues E176 and E275, and place the phenyl group in the hydrophobic pocket, formed by Y244, Y307, and Y316. An edge-to-face  $\pi$ - $\pi$  stacking of the phenyl group with Y244 is clearly evidenced (Figure 9, bottom panel).

STD-NMR experiments were designed to confirm our docking results. Comparing derivatives **1–3** spectra (Figure 4), the highest signal intensity for all protons from **3**

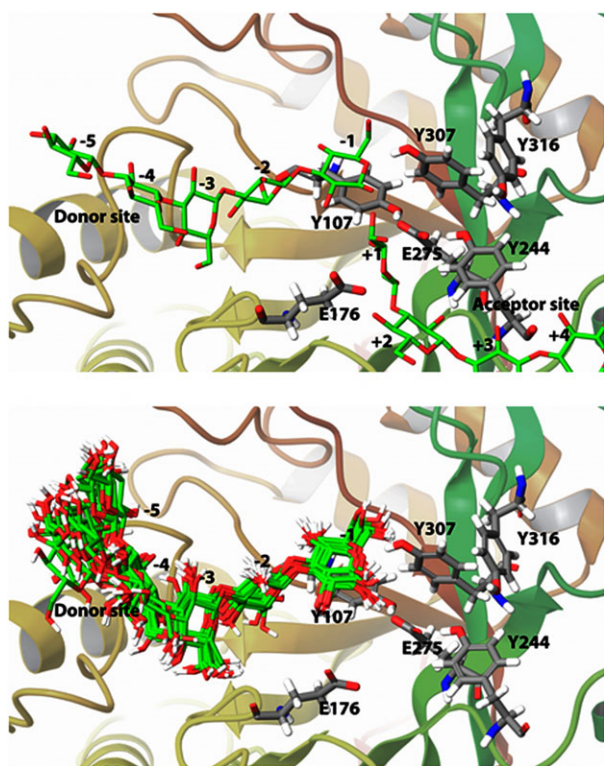


**Figure 8:** Close-up view of the ScGas2 crystal structure in complex with G5 (top panel), and the minima energy poses calculated for the complex within a 1 kcal/mol energy difference (bottom panel).

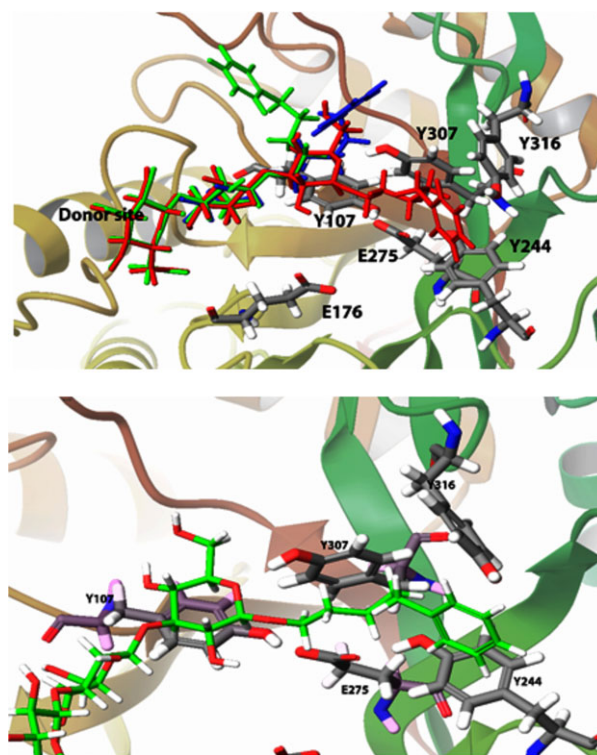


**Figure 9:** Most representative poses for compounds **1** (blue), **2** (green), and **3** (red) bounded to ScGas2 (top panel). Close-up view of the compound **3** docked into the active site of ScGas2 (bottom panel).

clearly indicates that its affinity is higher than the other two glycomimetics. Besides, regarding the relative intensities between the aglycone protons and the carbohydrate signals, it can be inferred that the phenylpentyl group is the anchoring moiety that enhances the interaction with the protein. STD-NMR experiments with mutants confirm this hypothesis. The complete loss of STD signal observed for Y244Q mutant (Figure 5, trace B) demonstrates the interaction of phenyl group with the tyrosine-rich pocket, in particular the proposed  $\pi$ - $\pi$  stacking with precisely Y244. In the case of Y107Q mutant (Figure 5, trace C), only phenylpentyl group interaction remains, meaning the loss of the carbohydrate moiety interaction. These experimental studies support the binding mode of compound **3** that is inferred from docking and previous STD-NMR studies.

Tryptophan fluorescence studies confirm that compounds **1** and **2** have a very low affinity and that compound **3** is the best compound of our series, showing a  $K_d$  of  $800 \pm 100 \mu\text{M}$ . This value is significant as affinity of ScGas2 with its own substrates is so low that it cannot be measured, so the introduction of the aromatic moiety, conveniently linked to laminaritrifose, has been able to increase the affinity, probably, an order of magnitude.

The inhibition assay let us confirm that glycomimetic **3** is able to bind the active site of ScGas2 better than a substrate as laminarihexaose. Unfortunately, the IC50 value is too high to consider **3** as a good inhibitor. It is also remarkable that no hydrolysis of compound **3** occurs in presence of ScGas2.

## Conclusions

These studies open a door for a rational design of compounds that could inhibit ScGas2 and close homologues such as *Aspergillus fumigatus* Gel4, that in turn is a drug target for Aspergillosis. We clearly demonstrate that a minimum of three monosaccharide units are required for ensuring a correct recognition at the donor binding site of the enzyme, and that the correct orientation of the hydrophobic radical toward the hydrophobic pocket increases the affinity of the ligand. This is supported by STD-NMR experiments that suggested that the hydrophobic radical acts as an 'anchoring moiety' for the glycomimetics. Also, from the docking studies, it appears that the representative poses present a CH- $\pi$  interaction between the phenyl group and residue Y244. STD-NMR experiments also showed that the affinities observed with wild-type ScGas2 are completely lost with the corresponding mutants Y107Q and Y244Q, thus confirming the specific interactions between these residues and the sugar at position -1 and the hydrophobic radical. Fluorescence studies and inhibition experiments also confirmed the above results. Further design of other trisaccharide analogues bearing other groups at the anomeric center of residue -1 is currently being pursued, and they will be reported in due course.

## Acknowledgments

This study was supported by the Ministerio de Economía y Competitividad (MINECO) and FEDER Program (Madrid, Spain, projects CTQ2013-44367-C2-1-P and CTQ2013-44367-C2-2-P), and the Gobierno de Aragón (Zaragoza, Spain. Bioorganic Chemistry group E-10 and Protein Targets group B-89). We acknowledge the Institute of Biocomputation and Physics of Complex Systems (BIFI) at the University of Zaragoza for computer time at clusters Terminus and Memento. E. M. and J. V.G. thank MEC for FPU and FPI predoctoral grants, respectively. The ARAID Foundation (Gobierno de Aragón, Spain) is also acknowledged for financial support.

## Conflict of Interest

The authors declare no conflict of interest.

## References

1. Desmet T., Soetaert W., Bojarova P., Kren V., Dijkhuizen L., Eastwick-Field V., Schiller A. (2012) Enzymatic glycosylation of small molecules: challenging substrates require tailored catalysts. *Chem Eur J*;18:10786–10801.
2. Desmet T., Soetaert W. (2011) Enzymatic glycosyl transfer: mechanisms and applications. *Biocat Bio-trans*;29:1–18.
3. Cantarel B.L., Coutinho P.M., Rancurel C., Bernard T., Lombard V., Henrissat B. (2009) The carbohydrate-active enzymes database (CAZy): an expert resource for glycogenomics. *Nucleic Acid Res*;37:D233–D238.
4. Reed P., Veiga H., Jorge A.M., Terrak M., Pinho M.G. (2011) Monofunctional transglycosylases are not essential for *Staphylococcus aureus* cell wall synthesis. *J Bacteriol*;193:2549–2556.
5. Lovering A.L., de Castro L.H., Lim D., Strynadka N.C. (2007) Structural insight into the transglycosylation step of bacterial cell-wall biosynthesis. *Science*;315:1402–1405.
6. Farkas V. (2003) Structure and biosynthesis of fungal cell walls: methodological approaches. *Folia Microbiol*;48:469–478.
7. Bowman S.M., Free S.J. (2006) The structure and synthesis of the fungal cell wall. *BioEssays*;28:799–808.
8. Engel J., Schmalhorst P.S., Routier F.H. (2012) Biosynthesis of the fungal cell wall polysaccharide galactomannan requires intraluminal GDP-mannose. *J Biol Chem*;287:44418–44424.
9. Lipke P.N., Ovalle R. (1998) Cell wall architecture in yeast: new structure and new challenges. *J Bacteriol*;180:3735–3740.
10. Orlean P. (1997) Biogenesis of yeast wall and surface components. In: Pringle J., Broach J., Jones E., editors.

- Molecular and Cellular Biology of the Yeast *Saccharomyces*. New York: Cold Spring Harbor Laboratory Press; p. 229–362.
11. Lutzen A., Wittmann V. (2004) Molecular basis of protein-carbohydrate interactions. *Highlights Bioorg Chem*; 119–123.
  12. Coutinho P.M., Henrissat B. (1999) Carbohydrate-active enzymes: an integrated database approach. In: Gilbert H.J., Davies G., Henrissat B., Svensson B., editors. *Recent Advances in Carbohydrate Bioengineering*. Cambridge, UK: Royal Society of Chemistry; p. 3–12.
  13. Hurtado-Guerrero R., Schüttelkopf A.W., Mouyna I., Ibrahim A.F.M., Shepherd S., Fontaine T., Latgé J.-P., van Aalten D.M.F. (2009) Molecular mechanisms of yeast cell wall glucan remodeling. *J Biol Chem*; 284:8461–8469.
  14. Hartland R.P., Fontaine T., Debeaupuis J.P., Simenel C., Delepierre M., Latgé J.P. (1996) A novel beta-(1-3)-glucanoyltransferase from the cell wall of *Aspergillus fumigatus*. *J Biol Chem*; 271:26843–26849.
  15. Hattori T., Kato Y., Uno S., Usui T. (2013) Mode of action of a  $\beta$ -(1 $\rightarrow$ 6)-glucanase from *Penicillium multicolor*. *Carbohydr Res*; 366:6–16.
  16. Couturier M., Roussel A., Rosengren A., Leone P., Stalbrand H., Berrin J.G. (2013) Structural and biochemical analyses of glycoside hydrolase families 5 and 26  $\beta$ -(1,4)-mannanases from *Podospira anserina* reveal differences upon manno-oligosaccharide catalysis. *J Biol Chem*; 288:14624–14635.
  17. Reid C.W., Legaree B.A., Auzanneau F.I., Clarke A.J. (2004) Inhibition of membrane-bound lytic transglycosylase B by NAG-thiazoline. *FEBS Lett*; 574:73–79.
  18. Scheurwater E., Reid C.W., Clarke A.J. (2008) Lytic transglycosylases: bacterial space-making autolysins. *Int J Biochem Cell Biol*; 40:586–591.
  19. Ostash B., Walker S. (2005) Bacterial transglycosylase inhibitors. *Curr Opin Chem Biol*; 9:459–466.
  20. Gastebois A., Fontaine T., Latgé J.P., Mouyna I. (2010) The  $\beta$ (1-3)glucanoyltransferase Gel4p is essential for *Aspergillus fumigatus*. *Eukaryot Cell*; 9:1294–1298.
  21. Fisher M.C., Henk D.A., Briggs C.J., Brownstein J.S., Madoff L.C., McCraw S.L., Gurr S.J. (2012) Emerging fungal threats to animal, plant and ecosystem health. *Nature*; 484:186–194.
  22. Goffeau A. (2008) Drug resistance: the fight against fungi. *Nature*; 452:541–542.
  23. Paiva J.A., Pereira J.M. (2013) New antifungal antibiotics. *Curr Opin Infect Dis*; 26:168–174.
  24. Perfect J.R., Andes D. (2013) Antifungal therapy: current concepts and evidence-based management. *Curr Med Res Opin*; 29:289–290.
  25. Regazzi M., Billaud E.M., Lefeuvre S., Stronati M. (2012) Pharmacokinetics of antifungal agents in neonates and young infants. *Curr Med Chem*; 19: 4621–4632.
  26. Scott L.J. (2012) Micafungin: a review of its use in the prophylaxis and treatment of invasive *Candida* infections. *Drugs*; 72:2141–2165.
  27. Pikman R., Ami B.-R. (2012) Immune modulators as adjuncts for the prevention and treatment of invasive fungal infections. *Immunotherapy*; 4:1869–1882.
  28. Armstrong-James D., Harrison T.S. (2012) Immunotherapy for fungal infections. *Curr Opin Microbiol*; 15:434–439.
  29. Vandeputte P., Ferrari S., Coste A.T. (2012) Antifungal resistance and new strategies to control fungal infections. *Int J Microbiol*; 2012:713687.
  30. Marca E., Valero-Gonzalez J., Delso I., Tejero T., Hurtado-Guerrero R., Merino P. (2013) Synthesis of O- and C-glycosides derived from  $\beta$ -(1,3)-D-glucans. *Carbohydr Res*; 382:9–18.
  31. Frisch M.J., Trucks G.W., Schlegel H.B., Scuseria G.E., Robb M.A., Cheeseman J.R., Scalmani G. *et al.* (2009) Gaussian 09, Revision A.1. Wallingford CT: Gaussian, Inc.
  32. Friesner R.A., Banks J.L., Murphy R.B., Halgren T.A., Klicic J.J., Mainz D.T., Repasky M.P., Knoll E.H., Shaw D.E., Shelley M., Perry J.K., Francis P., Shenkin P.S. (2004) Glide: a new approach for rapid, accurate docking and scoring. 1. Method and assessment of docking accuracy. *J Med Chem*; 47:1739–1749.
  33. Halgren T.A., Murphy R.B., Friesner R.A., Beard H.S., Frye L.L., Pollard W.T., Banks J.L. (2004) Glide: a new approach for rapid, accurate docking and scoring. 2. Enrichment factors in database screening. *J Med Chem*; 47:1750–1759.
  34. Friesner R.A., Murphy R.B., Repasky M.P., Frye L.L., Greenwood J.R., Halgren T.A., Sanschagrin P.C., Mainz D.T. (2006) Extra precision glide: docking and scoring incorporating a model of hydrophobic enclosure for protein-ligand complexes. *J Med Chem*; 49: 6177–6196.
  35. Meyer B., Mayer M. (1999) Characterization of ligand binding by saturation transfer difference NMR spectroscopy. *Angew Chem Int Ed*; 38:1784–1788.
  36. Angulo J., Nieto P. (2011) STD-NMR: application to transient interactions between biomolecules—a quantitative approach. *Eur Biophys J*; 40:1357–1369.

## Supporting Information

Additional Supporting Information may be found in the online version of this article:

**Appendix S1.** Graphical data of inhibition assays.